Numerical Optimization of an Organic Rankine Cycle Scheme for Co-generation

Fabrizio Naccarato*, Marco Potenza*‡, Arturo de Risi*, Giambattista Stigliano**

* Department of Engineering for Innovation, University of Salento Via Monteroni, 73100 - Lecce - Italy

** Laboratorio KAD3, Research Organization Contrada Baione, 70043 - Monopoli (BA) - Italy

(marcpote@tiscali.it, fabrizio.naccarato@libero.it, arturo.derisi@adrconsulting.it, g.stigliano@laboratoriokad3.com)

‡Corresponding Author; Marco Potenza, via Monteroni - 73100 Lecce - Italy, Tel: +39 0832 297782, Fax: +39 0832 297777, marcpote@tiscali.it

Received: 28.04.2014 Accepted: 13.06.2014

Abstract- The aim of the present work was the optimization of a small size Organic Rankine Cycle (ORC) system powered by a linear Parabolic Trough Collector (PTC) solar field; a numerical model code was developed on purpose. In the proposed scheme the solar energy is collected by a newly designed low cost PTC of 20m^2 with a single tracking axis and is concentrated on an opaque pipe collector in which flows as thermal fluid Therminol® 66 oil. An oil-free scroll expander coupled with a 2kW electrical generator is used to convert fluid energy into electrical energy. Cogeneration is performed by accumulating the waste in a double effect tank for domestic hot water (DHW) and heating. The use of cogeneration improves the global efficiency of the system from about 12% up to 30%. The numerical model implements the primary and secondary circuit as well as a detailed model of the PTC and the scroll expander. Real weather data of Brindisi (Italy) is considered to estimate and to optimize the performance of the plant. The system control has been optimized with the numerical model based on a multi objective genetic algorithm to increase the performance of the expander with the development of energy-save strategies.

Keywords ORC, Scroll expander, PTC, Cogeneration, Optimization.

1. Introduction

1. The interest for renewable energy working with fluids at low temperatures has increased in recent years, due to the increased interest in energy issues. Several solutions have been proposed to generate combined electric energy and hot water for domestic purpose, such as low size thermal solar plant [1], the use of engine exhaust heat recovery [2] and the geothermal heat source [3]. Among all the solution, the Organic Rankine Cycle is widely used [4, 5, 6]. In the ORC systems an organic working fluid with a boiling temperature lower than the water is used. Usually, the used heat source can be the collected solar energy that vaporized the organic fluid into an evaporator heat exchanger [7]. Vapour pressure decrease through an expander (turbine, scroll, screw or vane type) [8] connected with an electricity generator. The technical feasibility of ORC application in low temperature utilization has already been investigated and validated [9, 10, 11, 12]. Experimental studies on ORC units demonstrated that, for low power systems, the scroll expander is a good compromise between performance, high reliability and cost reduction [13, 14]. Moreover conventional scroll compressors can be easily converted into expanders [15]. The choice of the working fluid is important for the cycle optimization and for a raising in scroll performance. Several studies have been carried out on ORC working fluid selection due to theirs important role in system efficiency and on environmental impact [16, 17]. The fluid choice is influenced by several parameters, such as the thermal stability (to avoid degradation during working conditions), the compatibility with the circuit components and, above all, the thermodynamics characteristics which influence the temperature of the heating fluid and, subsequently, the dimensions of the solar plant [18]. In this paper a numerical model of a co-generative system realized by a solar power plant coupled with an ORC system was developed. In

Fig. **1** the power plant layout is reported.

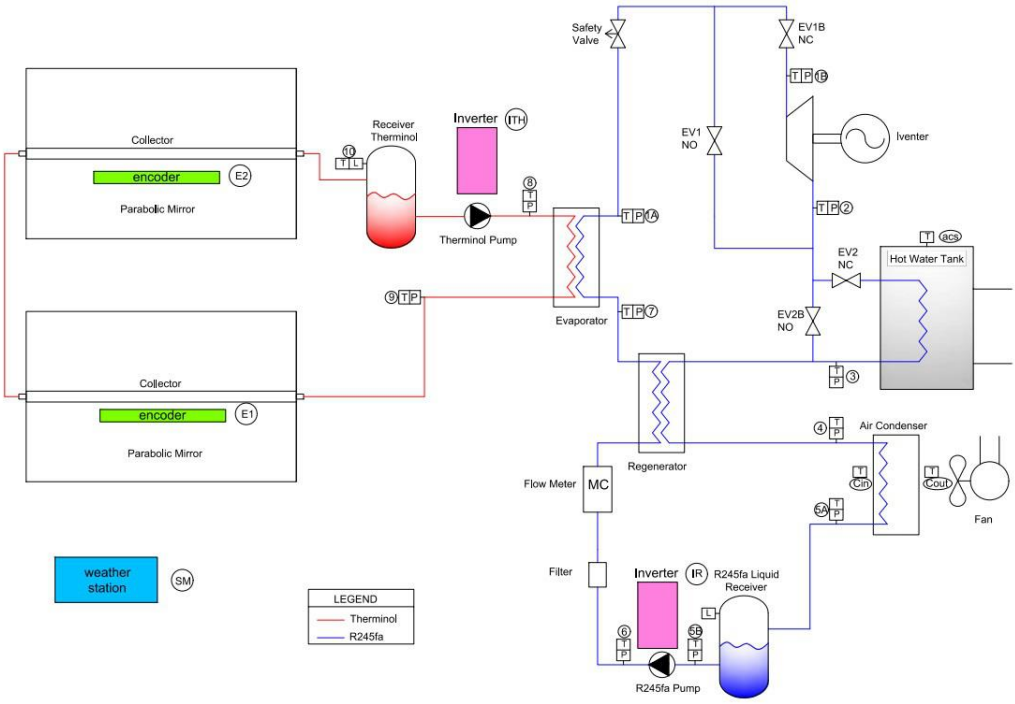

Fig. 1. Power plant layout

The simulated solar plant was a parabolic trough collector field with Therminol66 circulating in the receiver. A scroll working with R245fa fluid was used as expander. The NIST Reference Fluid Thermodynamic and Transport Properties Database (REFPROP) was used to determine the R245fa property in each working condition. The aim of the work was the optimization of the thermodynamic cycle to increase efficiency and the produced power by means of a genetic algorithm. Attention was focused on fluids working temperature. The developing of a model simulating a real plant is quite complex as the whole system is composed by several sub model each corresponding to a single component but connected with the others through thermodynamics variables (temperature, pressure, flow rate). Two different sections have been developed in the power plant: the ORC and the solar field thermodynamically connected by means of the evaporator. Models have been created and integrated in a main simulation code for each component. From a programming point of view, the main code executes a call to each module of components at each iteration. The simulation model allows evaluating a priori the criticism of each component as it is possible to calculate the thermodynamics variables, the working point and the transient conditions. The optimization step through a multi objective genetic algorithm, moreover, allows the identification of the best operative working points to obtain the maximum output power from the scroll with a reduction of testing time. The realized model has been tested on real weather data of solar radiation and ambient temperature. Below a description of the developed model for each component will be proposed.

2. Scroll expander model

The scroll model has been designed using a zero-dimensional model of an expanders scroll based on a compressor model [19, 20, 21, 22, 23]. The expander model consists of different phases, each corresponding to a thermodynamics change of the fluid from the inlet supply to the outlet of the expander, as summarized below:

1) Supply adiabatic expansion ***su→su,1***
2) Supply isobaric cooling **su,1→su,2**
3) Isentropic expansion due to volume ratio ***su,2→ad***
4) Adiabatic expansion at fixed volume ***ad → ex,2***
5) Adiabatic mixing between suction flow and leakage flow ***ex,2 → ex,1***
6) Exhaust cooling ***ex,1 → ex***

For each phases, a simulation cycle has been developed in order to predict the whole device behaviour and to test the ORC system at different thermodynamics conditions. In the following sections each single expander step modelling will be discussed.

2.1. Supply adiabatic expansion

During the suction phase it can be observed a pressure loss due to the inlet cross section reduction and to fluid leakage through the area of the volutes not covered by the seals. The pressure reduction can be considered as an adiabatic expansion through the section A_{su}. From the equations of mass and energy conservation through the nozzle, the mass flow rate can be written as:

$$\dot{M} = \frac{A_{su}}{v_{thr,su}} \sqrt{2(h_{su} - h_{thr,su})} \quad (1)$$

in which *thr,su* conditions can be calculated by means of a computing iterative, knowing the scroll supply mass flow rate and assuming a constant value for the entropy.

2.2. Inlet and outlet heat exchange

The heat exchange into the scroll can be summarized into three different components: the heat exchange between the working fluid and the inlet-outlet ducts; the exchange between the fluid and the scroll volutes; the heat transfer among the scroll walls and the external ambient. For the modelling of the heat exchange, it can be introduce a temperature of the scroll walls T_w and the exchanged power can be written as:

$$\dot{Q}_{su} = \dot{M}(h_{su,1} - h_{su,2}) = \left[1 - e^{\left(-\frac{AU_{su}}{\dot{M} C_p}\right)}\right] \dot{M} C_p (T_{su,1} - T_w) \quad (2)$$

The thermal heat exchange coefficient can be expressed by Reynold's analogy for a turbulent flow through a pipe and can be expressed as:

$$AU_{su} = AU_{su,n} \left(\frac{\dot{M}}{\dot{M}_n}\right)^{0.8} \quad (3)$$

Equation (3) can be applied both at the inlet and the outlet.

2.3. Scroll leakage

The leakage flow rate has been evaluated by means of the pressure analysis into the scroll and can be divided in two different contributes: leakage through the seals and leakage in the gap between the volute and the scroll walls (see Fig. 2) [24].

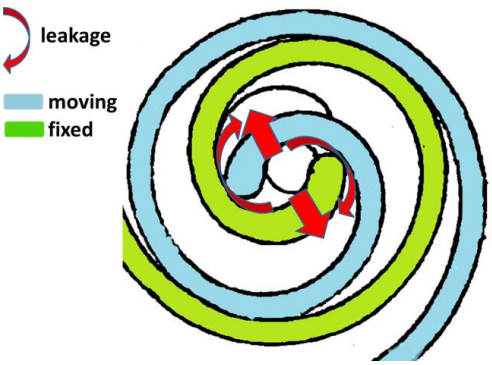

Fig. 2. Fluid leakage through parts of the scroll

It was assumed that the leakage flow rate can be computed by an adiabatic expansion into a nozzle through a reference section A_{leak} equal to the sum of all leakage areas. The throat pressure corresponds to the maximum between exhaust and critical pressure of the nozzle and is calculated by relation (4):

$$P_{crit,leak} = P_{su,2} \left[\left(\frac{2}{\gamma+1}\right)^{\left(\frac{\gamma}{\gamma+1}\right)}\right] \quad (4)$$

The mass flow rate can be calculated by means of equation (5):

$$\dot{M}_{leak} = \frac{A_{leak}}{v_{thr,leak}} \sqrt{2(h_{su} - h_{thr,leak})} \quad (5)$$

The effective mass flow rate can be written as the sum of two different contribution given by equations (1) and (5), as reported below:

$$\dot{M} = \dot{M}_{in} + \dot{M}_{leak} = \frac{NV_{s,\exp}}{v_{su,2}} + \dot{M}_{leak} \quad (6)$$

2.4. Inner expansion power

The organic working fluid into the scroll is characterized by three different phases: suction, expansion and discharge. The first phase begins when the moving part opens the suction port while the second occurs when the suction port is closed. The discharge phase starts when the moving part opens the discharge line. The total internal power is given by the sum of the three contributes of the following relation:

$$\dot{W}_{in} = \dot{W}_{suc} + \dot{W}_{\exp} + \dot{W}_{dis} = \dot{M}_{in}(h_{su,2} - h_{ex,2}) \quad (7)$$

where suction power, expansion power and discharge power can be written as:

$$\dot{W}_{suc} = \dot{M}_{in}(h_{su,2} - u_{su,2}) = \dot{M}_{in} P_{su,2} v_{su,2} = P_{su,2} \dot{V}_{s,\exp} \quad (8)$$

$$\dot{W}_{\exp} = \dot{M}_{in}(h_{su,2} - P_{su,2} v_{su,2} - h_{ad} + P_{ad} v_{ad}) \quad (9)$$

$$\dot{W}_{dis} = -r_{v,in} P_{ex,2} \dot{v}_{s,\exp} \quad (10)$$

It can be introduce the power loss due to friction $\dot{W}_{loss}$ and thus the shaft power can be expressed as:

$$\dot{W}_{sh} = \dot{W}_{in} - \dot{W}_{loss} = \dot{W}_{in} - 2\pi N_{rot} T_{loss} \quad (11)$$

2.5. Power balance and efficiency

From the power balance at the inlet and outlet of the scroll it can be written that the sum of all power terms is null:

$$\dot{W}_{loss} - \dot{Q}_{ext} + \dot{Q}_{su} - \dot{Q}_{amb} = 0 \quad (12)$$

where $\dot{Q}_{amb}$ is the power term lost from scroll to the external environment and can be expressed by the following relation:

$$\dot{Q}_{amb} = AU_{amb}(T_w - T_{amb}) \quad (13)$$

The isentropic efficiency of the expander is defined by the following relationship:

$$\varepsilon_S = \frac{\dot{W}_{sh}}{\dot{M}(h_{su} - h_{\exp})} \quad (14)$$

In order to evaluate the real working condition of the scroll, a numerical model of the rotor inertia and of the drag force of the electrical generator has been introduced. The model is based on the numerical implementation of the differential equation of dynamic expressed by:

$$J\frac{d^2\omega}{dt^2} + b\frac{d\omega}{dt} = T_{sh} \quad (15)$$

3. Heat exchangers model

An evaporator heat exchanger between the thermal storage and the ORC cycle has been inserted in the prototype layout. The evaporator transfers the heat from the hot source to the organic fluid (R245fa in the present work) up to its complete evaporation at the working pressure. Therefore into the heat exchanger three different zones can be defined: zone with liquid phase, zone with vapour phase and zone with a simultaneous coexistence of both phases. In order to create a numerical model of the evaporator able to evaluate the fluid inlet temperature, outlet temperature and power exchanged, it was used the logarithmic mean method, as suggested by Çengel et al. [25]. The model was developed using the following relations referred to the organic fluid and the hot fluid (Therminol66):

$$\dot{Q}_{ev,R245fa} = \dot{M}_{ev}(h^{in}_{ev,R245fa} - h^{out}_{ev,R245fa}) \quad (16)$$

$$\dot{Q}_{ev,Th} = \dot{M}_{ev}(h^{in}_{ev,Th} - h^{out}_{ev,Th}) \quad (17)$$

$$\dot{Q}_{ev,ml} = A_{ev}U_{ev}\Delta T_{ml} \quad (18)$$

where the logarithmic mean temperature ΔT_{ml} can be written as:

$$\Delta T_{ml} = \frac{\Delta T_1 - \Delta T_2}{\ln\frac{\Delta T_1}{\Delta T_2}} \quad (19)$$

$$\Delta T_1 = T^{in}_{ev,Th} - T^{out}_{ev,R245fa} \quad (20)$$

$$\Delta T_2 = T^{in}_{ev,R245fa} - T^{out}_{ev,Th} \quad (21)$$

Equations (16,17 e 18) have been iteratively resolved by increase the fluid enthalpy until the gap between the power calculated through the logarithmic temperature and the power calculated by enthalpy is lower than 10W:

$$err\dot{Q}_{ev} = \dot{Q}_{ev,ml} - \dot{Q}_{ev,R245fa} = \dot{Q}_{ev,ml} - \dot{Q}_{ev,Th} \le 10W \quad (22)$$

The enthalpy increase equation is defined by the following relation:

$$dh = e^{\left(\frac{err\dot{Q}_{ev}}{100\left(20-\dot{M}_{ev}\right)}\right)} \quad (23)$$

in which there is an exponential decrease of increment with the error reduction. In this way an accurate convergence value can be reached in acceptable computing time. Another component inserted into the layout is the heat recuperator that allows pre-heat the organic fluid before the evaporator and to recovery a portion of heat dissipated into the condenser. The model has been developed using the same principle used for the evaporator. The condenser is an air-fluid exchanger and is positioned after the scroll that allows a condensation of the R245fe fluid. In this case a distinguish have to be done between the vapour state liquid state of the organic fluid. The approach to evaluate the organic fluid temperature is the same described before for the evaporator.

4. Pump model

The working fluid pump is an important element in the layout as represents the driving force of the ORC system. The numerical model of the pump has been developed upon the hypothesis that the discharge pressure is equal to the total pressure loss on the line. There are some pressure losses into the refrigerant circuit related to curves, valves, heat exchanger and the pipe line. Moreover the expansion of fluid in the scroll can be expressed as a pressure reduction. All these effects have to be balanced by the driving force of the pump; the discharge pressure was imposed to be higher than the pipes line losses. However, both limit of maximum pressure and flow rate have been imposed into the model according the characteristic curve of a commercial pump. The pump is installed into the layout after the condenser where, generally, the refrigerant presents a bi- phase composition. Therefore in the model the flow rate contribution both of liquid and vapour phase have been considered. The volumetric flow rate for liquid and vapour phases can be calculated by the following equation.

$$\dot{M}_{pump,l} = \dot{V}_s N(1 - x_v) \quad (24)$$

$$\dot{M}_{pump,v} = \dot{V}_s N(x_v) \quad (25)$$

The power transferred to the fluid can be obtained by:

$$\dot{W}_{pump,l} = \frac{\dot{M}_l\left(P_{pump,out} - P_{pump,in}\right)}{\eta_{pump,l}} \quad (26)$$

$$\dot{W}_{pump,v} = \frac{\dot{M}_v\left(P_{pump,out} - P_{pump,in}\right)}{\eta_{pump,v}} \quad (27)$$

η_l and η_v are the pump efficiency for liquid and vapour phase respectively. Into the model a PI controller regulating the pump engine speed as function of the refrigerant temperature at the evaporator outlet has been inserted.

5. Thermal storage model

Two different thermal storages have been inserted into the layout: the Therminol® storage and the domestic hot water tank (DHW). The thermal storages model is based on thermal inertia through a mass balance and energy that can be expressed by:

$$U_{in} = U_{acc} - U_{dis} \tag{28}$$

that can be re-written as:

$$C_p \dot{M}_{in}\left(T_{acc,in} - T_{acc,out}\right)\ dt = C_p M_{acc}\left(T_{acc} - T_{acc,out}\right) - h_{acc} A_{acc}\left(T_{acc,out} - T_{amb}\right) \tag{29}$$

From equation (29), the temperature of the thermal storage equal to the storage outlet $T_{acc;out}$ can be calculated.

6. PTC model

The parabolic trough collector model was developed considering the system composed by the receiver positioned in the focus of the parabolic linear collector [26]. In Fig. 3 a section of the receiver tube is reported.

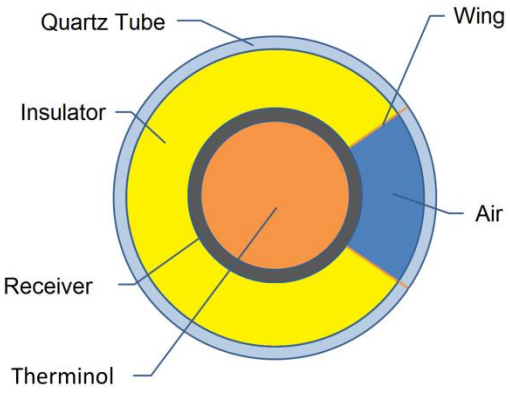

Fig. 3. PTC receiver section

The internal part of the receiver is realized by a steel pipe surrounded by a thermal insulator for about 270°C radials. The outer part is realized with a glass tube. The light reflected and collimated by the parabolic collector enters the receiver from the opposite side with respect to insulator and heat the steel pipe and, subsequently, the working fluid flowing. The insulator and the glass pipe reduce the heat loss due to convection and the radiation with the external air. The receiver heat loss can be analyzed by assuming several contribute, such as the radiation, the internal and external pipe convection and the exchange between the steel and the glass. The total power supplied by the PTC system can be calculated by the following relation:

$$\dot{Q}_{PTC} = F_R\, A_a \left[S_{sun} - \frac{A_r}{A_a} U_L (T_{Th} - T_{amb}) \right] \tag{30}$$

where the receiver and collector geometry factor A_r e A_a have been considered related to the power loss by the receiver F_R:

$$F_R = F' F'' \tag{31}$$

where F' can be written as:

$$F' = \frac{1/U_L}{\frac{1}{U_L} + \frac{D}{h_{fi} D_i} + \left(\frac{D}{2k} ln \frac{D}{D_i} \right)} \tag{32}$$

h_{fi} is the liminal exchange coefficient between Therminol® and the steel pipe while U_L is the global exchange coefficient of the receiver:

$$U_L = \left[\frac{A_r}{\left(h_w + h_{r,c-a}\right) A_a} + \frac{1}{h_{r,r-c}} \right]^{-1} \tag{33}$$

where $h_{r,c-a}$ is the radiation coefficient and $h_{r,r-c}$ is the exchange coefficient between the receiver and the glass tube. The F'' coefficient, instead, can be calculated by relation (34):

$$F'' = \frac{\dot{M}_{Th} C_p}{A_r U_L F'} \left[1 - exp\left(- \frac{A_r U_L F'}{\dot{M}_{Th} C_p} \right) \right] \tag{34}$$

The power of receiver can be calculated by equation (30) by knowing the collector and receiver geometry and the incident solar radiation. In the model, solar radiation was obtained by historical data from ENEA [27].

7. Results

In this section results from numerical simulations working with an experimental solar radiation profile have been reported. In order to optimize the model in a steady state and to evaluate the performance of the heat recovery exchanger, the DHW storage was not considered. During the first few iteration of simulation, the ORC plant is powered off and the scroll does not produce energy. All the solar radiation from the collectors allows the Therminol® storage temperature increase up to 140°C. At this point the outlet temperature of the evaporator in the R245fa side is enough to start the organic fluid pump and subsequently the scroll, thus allowing energy production. In Fig. 4 inlet and outlet temperature of the evaporator as function of the daily time expressed in hours has been reported.

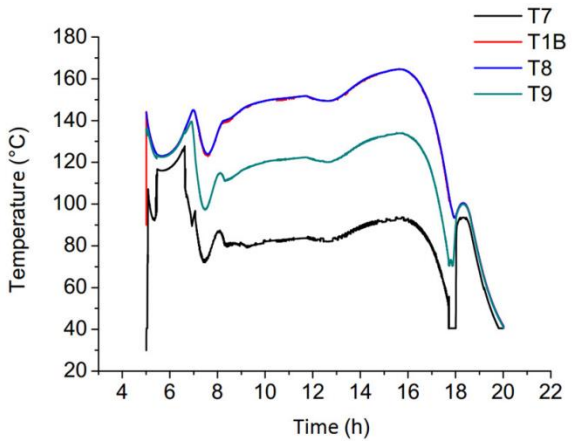

Fig. 4. Inlet and outlet temperature of the evaporator;

T1B is the ORC side outlet temperature, T9 is the PTC side outlet temperature, T8 is the inlet temperature from the Therminol thermal storage and T7 ORC side inlet temperature.
In the first hours of day when solar radiation is low, a temperature reduction due to heat consumption from the Therminol® storage can be observed. The maximum temperature of Therminol® is about 165°C, corresponding to the maximum value of T_8 e T_{1B}. These temperatures are very close due to the high efficiency andheat exchange of the selected evaporator (341W/m^{2}C). In Fig. 5 the heat recovery temperature behaviour has been reported.

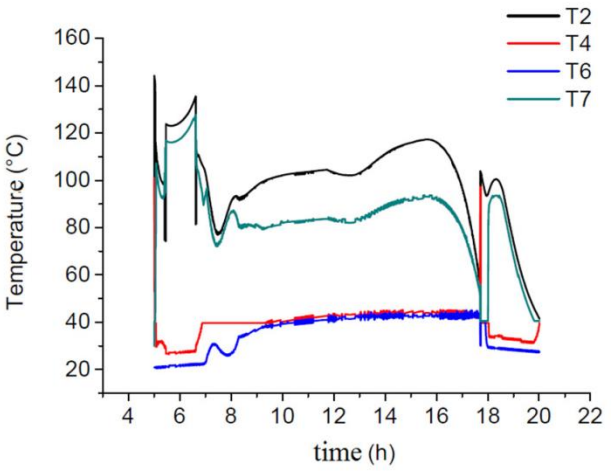

Fig. 5. In and out temperature of the heat recovery Exchanger

T2 is the ORC side inlet vapour temperature, T6 is the ORC side inlet liquid temperature, T4 is the ORC side outlet vapour temperature, T7 is the ORC side outlet liquid temperature

Outlet temperatures of fluid at high and low pressure have a similar behaviour of the system load curve. A constant value of ORC outlet temperature can be observed due to the biphasic condition of the fluid. In Fig. 6 the temperature behaviour at the scroll inlet and outlet is shown.

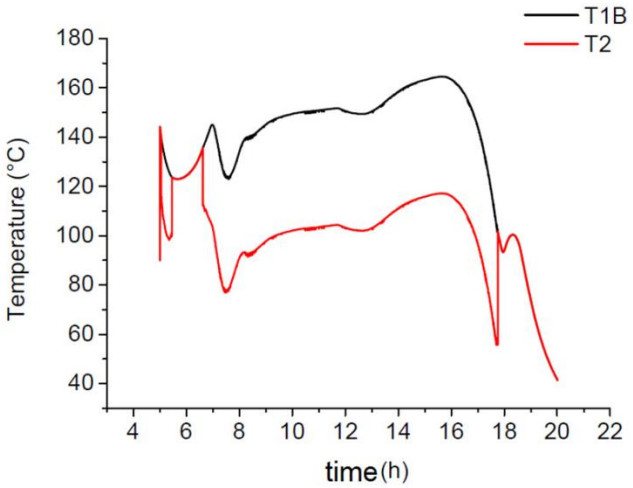

Fig. 6. Inlet and outlet temperatures from scroll

In Fig. 7 the mass flow rate of ORC and PTC circuits are reported. In the Therminol® pump model a PI controller with an objective temperature of 140°C has been inserted. The Therminol® mass flow in steady state is about 0,18kg/s while the R245fa organic fluid is of 0,055kg/s. These values have been limited according to pumps datasheet.

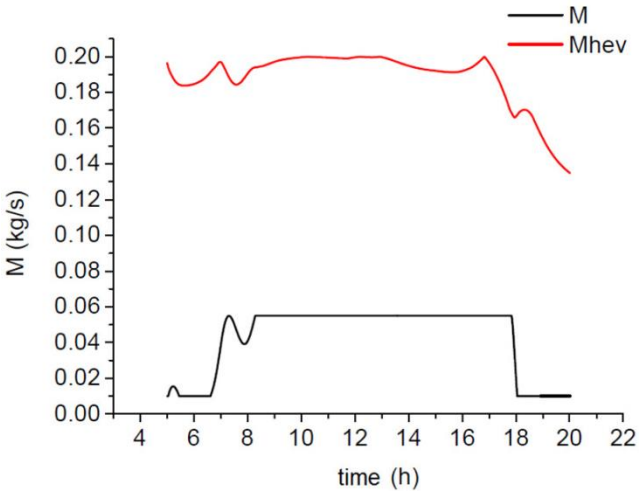

Fig. 7. Mass flow rate for PTC and ORC circuit

In Fig. 8 is reported the power behaviour of the heat exchangers. In steady state conditions, about 11.5kW of thermal power are introduced in the system by the evaporator while the condenser dissipates about 10kW. The heat recovery exchanger regain about 4kW of thermal power that would otherwise be borne by the evaporator and condenser. The difference between the evaporator power and the condenser power is the thermal power absorbed by the scroll.

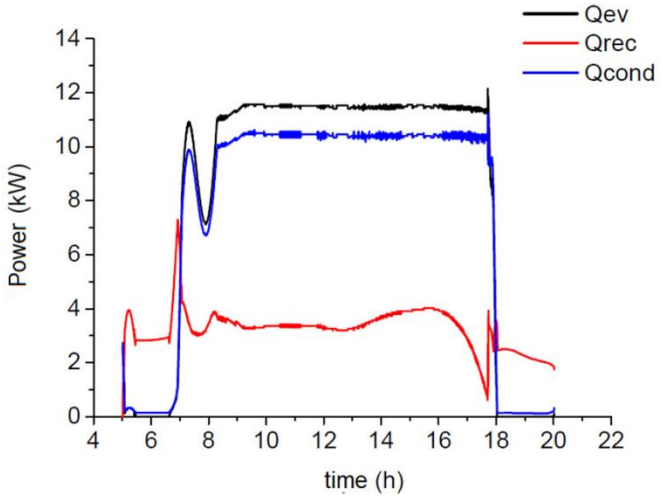

Fig. 8. Heat exchangers powers

In Fig. 9 the scroll shaft power W_{sh}, the number of revolutions N_{sh}, the calculated power for heat exchangers W_{therm} and the power absorbed by the pump W_{pp} expressed in W are reported. It can be underlined that pump power (less than 100W) is negligible with respect to the power produced by scroll (about 1.5kW).

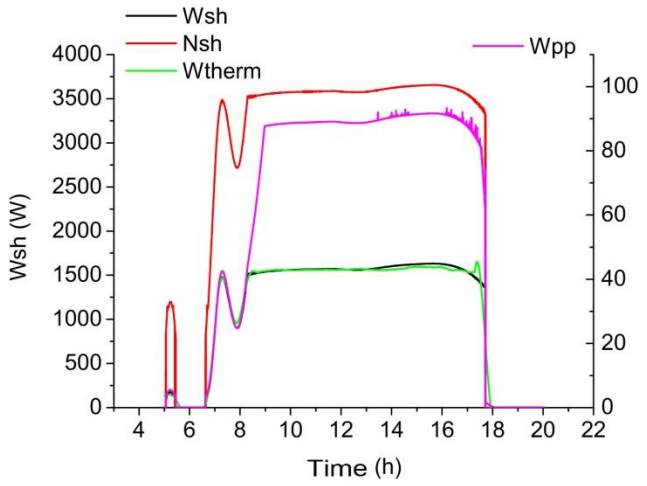

Fig. 9. Power delivered by the scroll, the rotational speed and the ORC pump power.

The thermal power and the effective power have the same behaviour with different values due to friction loss. In Fig. 10, the scroll and ORC cycle efficiency are reported. At full load the ORC cycle efficiency is about 0.09 while the scroll efficiency is about 0.6. The amount of produced energy at the scroll shaft is of 19kWh.

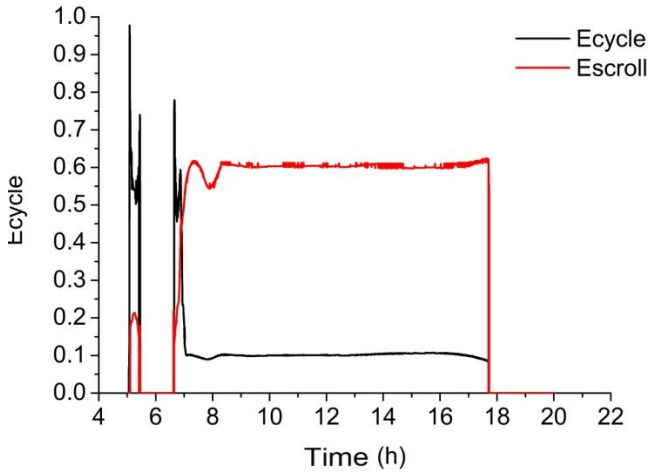

Fig. 10. Efficiency of the ORC cycle and the scroll

In order to increase the system efficiency and to determine the best working condition of the real plant, an optimization of the model was carried out by means of a multi objective genetic algorithm (MOGA).

A genetic algorithm (GA) is based on the similitude of math problem solving with the natural selection based on the assumption that the best individuals have a higher probability of surviving [28, 29]. In the GA an individual is defined as a numerical solution of the function to be maximized or minimized (called objective function). An individual is described by a binary string or D.N.A. The best individuals can maximize the function "better" than other. In the GA, starting from an initial population, new generations are created by combining the binary code of individuals using a crossover and a mutation. Some individuals are discarded because they exceed the limit imposed for the population. Best individuals of different generations can maximize the solution. When different objective functions have to be maximized, a MOGA optimization is used for global solutions in nonlinear problems detection [30]. In multi objective genetic algorithm there are several solutions that maximize the objective functions and can be identified by the Pareto filter that extracts non dominated solution from a set of individuals in order to make out the curve of the best solutions [31]. Once defined the system layout and after the choice of components in the ORC model, the optimization was carried out by maximizing the ORC cycle efficiency and the produced energy. As individuals for the GA have been used the scroll activation temperature and the set point temperature of Therminol® in the PTC circuit. In particular, into the model of genetic algorithm for the Solar-ORC plant a minimization of the reciprocal variables has been used. In relation (35) is reported the objective functions f_1 and f_2 to be minimize and the limits for the individuals of a population:

$$\min\left(f_1=\frac{1}{E(T_{1B},T_{10})},\ f_2=1-\eta(T_{1B},T_{10})\right) \tag{35}$$

$$\text{Subject to}\quad \begin{cases}110\le T_{1B}\le 160\\ 110\le T_{10}\le 180\end{cases}\ ^{\circ}C$$

In Fig. 11 the flow chart of the MOGA calculation has been reported.

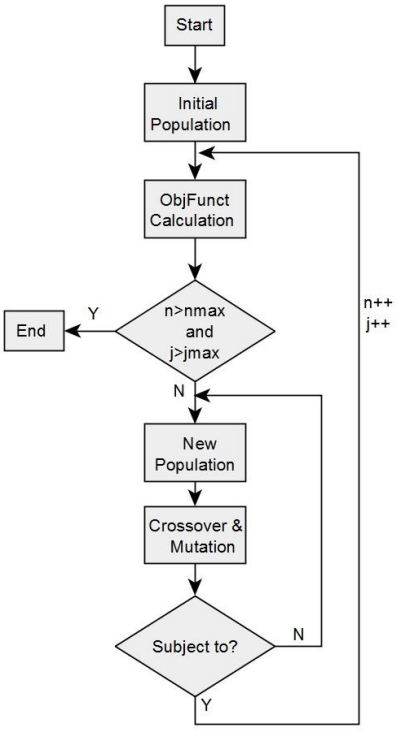

Fig. 11: MOGA flow chart for *n* populations and *j* generations

After the initialization with a random population, objective functions are calculated and a check on the maximum of iterations is performed. A new individual is generated by means of mutation and crossover of the binary string and a new calculation of objective functions are carried out. When the maximum value of the populations *n* and generations *j* is reached the algorithm is terminated and a pareto filtering is applied to the solutions. In the ORC multi objective genetic algorithm a starting population of candidate solution of 100 individuals with 5 generation was considered. In the ORC system, the optimization process has been performed using a standard solar radiation profile under the hypothesis of a constant radiation of 700 W/m^2.

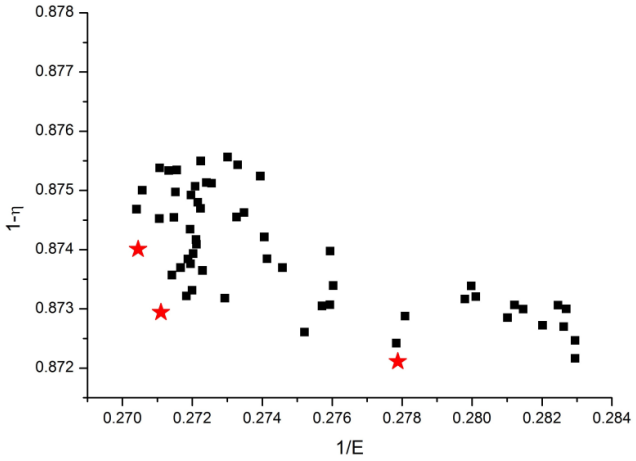

Fig. 12. Behaviour of the Pareto front

In Fig. 12 the individuals population and three individuals on the Pareto front (in red) are reported. The point on the Pareto front that optimize the system by minimizing the distance from the origin of the reference system, corresponds to an activation temperature of the scroll of 112°C and a value for the Therminol® temperature in the storage of 143°C. The optimized temperature values have been inserted into a new simulation of the model by using a real solar radiation profile. In Fig. 13 the ORC cycle and the scroll efficiency are reported while in Fig. 14 the output power at the scroll shaft is shown.

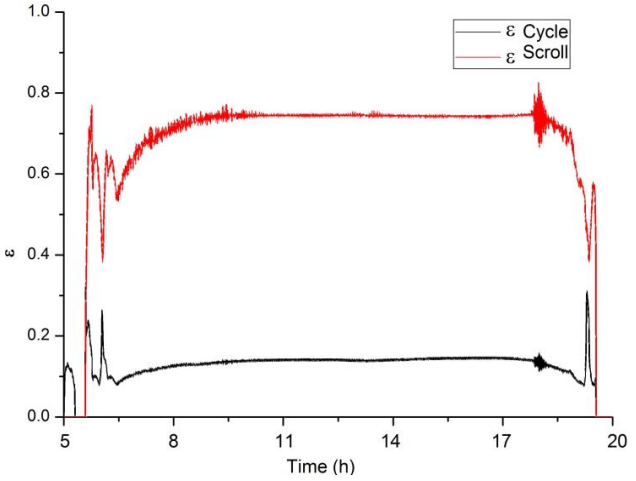

Fig. 13. Behaviour of the ORC cycle (black curve) and of the scroll efficiency (red curve)

After the optimization process the output power of the scroll is of about 2kW, greater than the value obtained without optimization (1.5kW) and reported in Fig. 9. The scroll efficiency is about 0.7 while the cycle efficiency increases up to 0.12 with respect to the un-optimized conditions reported in Fig. 10.

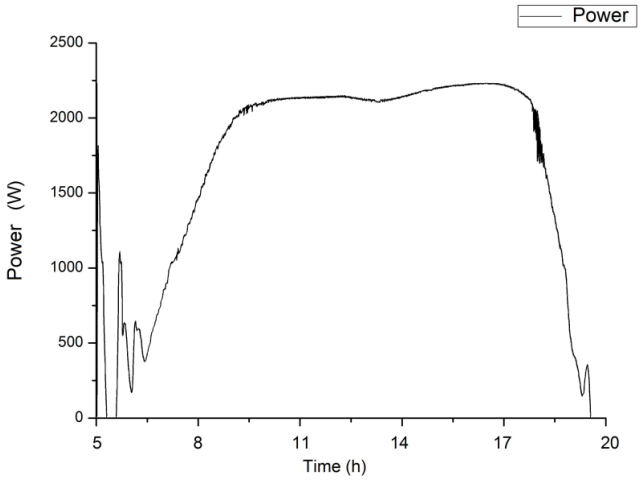

Fig. 14 Behaviour of the output power of the scroll

8. Conclusions

In the present work a complete model of a PTC plant coupled with an ORC system for combined energy and DHW production was developed. As expander machine a modified scroll compressor able to provide an electrical power up to 2kW was used. This condition can be reached by using an appropriate organic fluid, like the R245fa for the organic Rankine cycle, and by optimizing the working temperature. As working fluid for the parabolic trough collector the Therminol® 66 was chosen. Each component of the plant, such as heat exchangers and fluids pumps, was modelled in order to predict the real behaviour of the system. A detailed model of the scroll expanders was developed too. In particular the scroll model was divided in different phases each corresponding to a thermodynamic change. In this way it was possible to determine the mass flow rate processed into the expanders, the power and to evaluate the leakage loss. A particular receiver tube was developed and modelled in order to reduce the heat dissipation. Daily solar radiation behaviour from experimental data was used in the PCT simulation in order to check the system in real-like conditions. Once reached the convergence of the simulation, all the thermodynamics conditions of the system were obtained. The aim of the paper is to realize a model that simulates the plant and optimize the obtained results to maximize the efficiency of the ORC cycle and of the electrical power. The optimization was performed on the developed model by applying a multi objective genetic algorithm according to method proposed by Murata et all. [30]. Some researchers carried the optimization on the ORC cycle [32,33] or on the working fluid [34], without considering the whole power plant or the cycle efficiency.

In the present work a Therminol temperature and scroll activation temperature were used as parameters for the GA population. From a starting population of 100 individuals in 5 generation a well defined point on the Pareto front was identified, corresponding to a PTC fluid temperature of 143°C at the storage and of 112°C as scroll activation temperature.

The developed model optimized by means of a multi objective genetic algorithm can be used to reach the best operative conditions for the working fluids that optimize the efficiency of the system. As the model is based on real weather and radiations data, it can be calculated the real annual energy capability of the plant and an evaluation of the feasibility of the power plant can be made. Moreover the model is scalable so that it can be used for higher PTC solar field or for bigger scroll or it can be tested with different working fluids. By implementing different expander computational code, it is possible to use the model to check new configurations. Using the proposed simulation and optimization model it is possible to identify the best power plant configuration to maximize energy and hot water production for different solar radiation conditions, for different plant dimensions and for several applications such as domestic or industrial.

Acknowledgements

The innovative contents described in this paper are disclosed after the permission of OMP S.r.l. company, which committed to Laboratorio KAD3 S.c.a.r.l. the research project called "OL.COM. - Sviluppo di un sistema a ciclo Rankine a fluido organico (ORC) di piccola taglia per la produzione combinata di energia elettrica e termica da fonte solare", co-funded by Italian Government (Legge 12 luglio 2011, n. 106 – Credito di imposta per le imprese che finanziano progetti di ricerca in Università o enti pubblici di ricerca).

References

[1] D. J. Yang, Z. F. Yuan, P. H. Lee e H. M. Yin, «Simulation and experimental validation of heat transfer in a novel hybrid solar panel,» International Journal of Heat and Mass Transfer, vol. 55, p. 1076–1082, 2012.

[2] C. Aussant, A. S. Fung, V. I. Ugursal e H. Taherian, «Residential application of internal combustion engine based cogeneration in cold climate-Canada,» Energy and Buildings, vol. 41, p. 1288–1298, 2009.

[3] R. Gabbrielli, «A novel design approach for small scale low enthalpy binary geothermal power plants,» Energy Conversion and Management, vol. 64, p. 263–272, 2012.

[4] S. H. Gang, «Design and experimental study of ORC (organic Rankine cycle) and radial turbine using R245fa working fluid,» Energy, vol. 41, pp. 514-524, 2012.

[5] D. Manolakos, G. Kosmadakis, S. Kyritsis e G. Papadakis, «Identification of behaviour and evaluation of performance of small scale, low-temperature Organic Rankine Cycle system coupled with a RO desalination unit,» Energy, vol. 34, pp. 767-774, 2009.

[6] E. H. Wang, H. G. Zhang, Y. Zhao, B. Y. Fan, Y. T. Wu e Q. H. Mu, «Performance analysis of a novel system combining a dual loop organic Rankine cycle (ORC) with a gasoline engine,» Energy, vol. 43, pp. 385-395, 2012.

[7] A. M. Delgado-Torres e L. García-Rodríguez, «Analysis and optimization of the low-temperature solar organic Rankine cycle (ORC),» Energy Conversion and Management, vol. 51, p. 2846–2856, 2010.

[8] G. Qiu, H. Liu e S. Riffat, «Expanders for micro-CHP systems with organic Rankine cycle,» Applied Thermal Engineering, vol. 31, p. 3307, 2011.

[9] B. T. Liu, K. Chien e C. Wang, «Effect of working fluids on organic Rankine cycle for waste heat recovery,» Energy, vol. 29, p. 1207–1217, 2002.

[10] B. F. Tchanche, G. Lambrinos, A. Frangoudakis e G. Papadakis, «Low-grade heat conversion into power using organic Rankine cycles – A review of various applications,» Renewable and Sustainable Energy Reviews, vol. 15, p. 3963–3979, 2011.

[11] A. Schuster, S. Karellas, E. Kakaras e H. Spliethoff, «Energetic and economic investigation of Organic Rankine Cycle applications,» Applied Thermal Engineering, vol. 29, p. 1809–1817, 2009.

[12] D. Tempesti, G. Manfrida e D. Fiaschi, «Thermodynamic analysis of two micro CHP systems operating with geothermal and solar energy,» Applied Energy, vol. 97, pp. 609-617, 2012.

[13] H. Wang, R. Peterson e T. Herron, «Experimental performance of a compliant scroll expander for an organic rankine cycle,» Proceedings of the Institution of Mechanical Engineers Part A-Journal of Power and Energy, vol. 223, 2009.

[14] R. Zanelli e D. Favrat, «Experimental investigation of a hermetic scroll expander-generator,» in Proc. the Int. compressor engineering conference, Purdue, 1994.

[15] R. Shaffer, «Advanced scroll compressor, vacuum pump and expanders». USA Brevetto 189912a1, 08 2007.

[16] R. Rayegan e Y. X. Tao, «A procedure to select workingfluids for Solar Organic Rankine Cycles (ORCs),» Renewable Energy, vol. 36, pp. 659-670, 2011.

[17] A. B. Gozdur e W. Nowak, «Comparative analysis of natural and synthetic refrigerants in application to low temperature clausius rankine cycle,» Energy, vol. 32, p. 344–352, 2007.

[18] A. A. Lakew e O. Bolland, «Working fluids for low-temperature heat source,» Applied Thermal Engineering, vol. 30, p. 1262–1268, 2010.

[19] M. Kane, D. Larrain, D. Favrat e Y. Allani, «Small hybrid solar power system,» Energy, vol. 28, pp. 1427-1443, 2003.

[20] V. Lemort, S. Quoilin, C. Cuevas e J. Lebrun, «Testing and modeling a scroll expander integrated into an organic rankine cycle,» Applied Thermal Energy, vol. 29, pp. 3094-3102, 2009.

[21] S. Quoilin, V. Lemort e J. Lebrun, «Experimental study and modeling of an organic rankine cycle using scroll expander,» Applied Energy, vol. 87, pp. 1260-1268, 2010.

[22] E. Winady, C. Saavedra e J. Lebrun, «Experimental analysis and simplified modelling of a hermetic scroll refrigeration compressor,» Applied Thermal Energy, vol. 22, pp. 107-120, 2002.

[23] E. Winandy, C. Saavedra e J. Lebrun, «Experimental analysis and simplified modelling of a hermetic scroll refrigerant compressor,» Applied Thermal Energy, vol. 22, pp. 107-120, 2002.

[24] N. P. Halm, «Mathematical modeling of scroll compressors, Master Thesys,» in Purdue University, West Lafayette, IN, 1997.

[25] Y. A. Cengel e P. Ricciardi, "Termodinamica e trasmissione del calore- Elementi di acustica e illuminotecnica", MGraw-Hill companies, 2009.

[26] J. A. Duffie e W. A. Beckman, Solar Engineering of Thermal Processes, John Wiley & Sons, 2006.

[27] ENEA, www.solaritaly.enea.it., [Online].

[28] J.H. Holland, " Adaptation in natural and artificial systems ", MIT Press Cambridge, MA, USA 1992

[29] David E. Goldberg, "Genetic Algorithms in Search, Optimization & Machine Learning", Addison-Wesley, 1989

[30] Murata, T.; Ishibuchi, H., "MOGA: multi-objective genetic algorithms," Evolutionary Computation, 1995., IEEE International Conference on , vol.1, no., pp.289,, Nov. 29 1995-Dec. 1 1995

[31] Carlos M. Fonseca and Peter J. Fleming. "Genetic algorithms for multiobjective optimization: Formulationdiscussion and generalization". In Proceedings of the 5th International Conference on Genetic Algorithms, pages 416-423, San Francisco, CA, USA, 1993. Morgan Kaufmann Publishers Inc.

[32] Y. Dai, J. Wang, L. Gao, "Parametric optimization and comparative study of organic Rankine cycle (ORC) for low grade waste heat recovery", Energy Conversion and Management, vol 50, pagg 576-582, 2009

[33] E. Wang, H. Zhang, B. Fan and Y. Wu, "Optimized

performances comparison of organic Rankine cycles for low grade waste heat recovery", Journal of Mechanical Science and Technology 26, (2012) 2301-2312

[34] Z.Q. Wanga, N.J. Zhoub, J. Guo, X.Y. Wang, "Fluid selection and parametric optimization of organic Rankine cycle using lowtemperature waste heat", Energy, 40 (2012) 107-115